Ocean Sci. Discuss., 6, 1437–1475, 2009
www.ocean-sci-discuss.net/6/1437/2009/

Ocean Science Discussions

Papers published in *Ocean Science Discussions* are under open-access review for the journal *Ocean Science*

Barents Sea heat – transport, storage and surface fluxes

L. H. Smedsrud[1], **R. Ingvaldsen**[2,1], **J. E. Ø. Nilsen**[3,1], **and Ø. Skagseth**[2,1]

[1]Bjerknes Centre for Climate Research, Bergen, Norway
[2]Institute of Marine Research, Bergen, Norway
[3]Nansen Environmental and Remote Sensing Centre, Bergen, Norway

Received: 25 June 2009 – Accepted: 26 June 2009 – Published: 7 July 2009

Correspondence to: L. H. Smedsrud (larsh@gfi.uib.no)

Published by Copernicus Publications on behalf of the European Geosciences Union.

Abstract

Sensitivity of the Barents Sea to variation in ocean heat transport and surface fluxes is explored using a 1-D column model. Mean monthly ocean transport and atmospheric forcing are synthesised and force model results that reproduce the observed winter convection and surface warming and freshening well. Model results are compared to existing estimates of the ocean to air heat fluxes and horizontally averaged profiles for the southern and northern Barents Sea.

Our results indicate that the ~70 TW of heat transported to the Barents Sea by ocean currents is lost in the southern Barents Sea as latent, sensible, and long wave radiation, each contributing 23–39 TW to the total heat loss. Solar radiation adds 26 TW in the south, as there is no significant ice production.

The northern Barents Sea, the major part of the area, receives little ocean heat transport. This leads to a mixed layer at the freezing point during winter and significant ice production. There is little net surface heat loss in the north, the balance is achieved by long wave loss removing most of the solar heating, and the model also suggests a positive sensible heat gain.

During the last decade the Barents Sea has experienced an atmospheric warming and an increased ocean heat transport. Despite large changes the Barents Sea heat loss remains robust, the temperature adjusts, and the yearly cycle remains. Decreasing the ocean heat transport below 50 TW starts a transition towards Arctic conditions. The heat loss in the Barents Sea depend on the effective area for cooling, and an increased heat transport probably leads to a spreading of warm water further north.

1 Introduction

Despite being shallow and small, the Barents Sea is special because it dominates Arctic Ocean heat storage (Serreze et al., 2007). With a mean depth of ~230 m, and an area ~14% of the Arctic Ocean, more than 50% of the Arctic Ocean winter heat

OSD

6, 1437–1475, 2009

loss occur in the Barents Sea. This happens because the relatively large open water areas in the Barents Sea allows both large absorption of incoming solar radiation during spring and summer, and stronger heat loss in autumn and winter than the other Arctic Seas.

When other Arctic Seas freeze over and are insulated from further cooling, the southern Barents Sea remain open, and is convectively cooled to the bottom. In this way most of the ocean heat is lost every winter, and the Barents Sea remains open and coupled to the atmosphere. If this ocean heat was not re-supplied by advection, the Barents Sea surface would drift towards the freezing point after a few years, as will be demonstrated in this paper. Figure 1 shows the major ocean transport into, and out of, the Barents Sea as it will be presented here.

We will explore the relations between the ocean heat transport, the vertical heat fluxes, and the mean temperature field using a vertical column model. The term "ocean heat transport" will be used consistently for the horizontal advection of heat by the ocean currents. The term "heat flux" will be used for vertical exchange, i.e. air-sea-ice fluxes at the surface. Surface fluxes depend on vertical mixing and stratification, so it was also necessary to recapture a significant input of freshwater to the Barents Sea surface, and the advected net salt contribution.

In this study we present heat transports and fluxes using TW ($1\,\mathrm{TW}=1-10^{12}\,\mathrm{W}$). Individual vertical heat fluxes at the surface will sometimes be discussed using $\mathrm{W/m^2}$.

The two units are of a similar magnitude as the Barents Sea area is $1.3\times10^{12}\,\mathrm{m^2}$. Heat transport will be referenced to 0°C which is close to the temperature of the outflow to the Arctic Ocean (Schauer et al., 2002). Volume transport is given in Sv ($1\,\mathrm{Sv}=1-10^{6}\,\mathrm{m^3/s}$). Fluxes of freshwater are given in mSv ($1\,\mathrm{mSv}=10^{3}\,\mathrm{m^3/s}=31.5\,\mathrm{km^3/year}$). The relative contribution of the different freshwater sources is independent of a reference salinity, but we will use a reference salinity of 35.0 here. This is the middle value between 34.8, used for the Arctic Ocean (Aagaard and Carmack, 1989), and the inflow salinity of 35.2 across the Greenland-Scotland ridge (Dickson et al., 2007). The Barents Sea surface layer is often fresher than 34.8,

but at depth salinities approach 35.0.

A synthesis of the mean state of the Barents Sea is given in Sect. 2, including fluxes of heat and freshwater. Such a synthesis has not been found elsewhere, and is a necessity for the 1-D column model applied here. Model forcing, setup, and results are presented in Sect. 3. We then discuss sensitivity and some changes in forcing during the last decades in Sect. 4, before concluding on our findings.

2 Barents Sea mean state

Ocean advection has a strong influence on the Barents Sea mean state (Mosby, 1962). The main inflow area, the Barents Sea Opening (BSO), defines a warm area in the southwest between Norway and Bear Island (Fig. 1). Figure 2 shows that winter surface temperatures in the BSO lies around 5°C (Nilsen et al., 2008). The 0°C isotherm extend almost to the southern tip of Novaya Zemlya. During summer the 6°C isotherm almost reaches the southern tip of Novaya Zemlya, and the maximum temperatures in the BSO are 8–9°C (not shown). This means that the gross southern Barents Sea temperature gradient is similar all year, but stronger in winter than summer.

In the northern Barents Sea surface water is at freezing temperatures during winter (Fig. 2), increasing to 0–2°C during summer. Below the surface layer the mean salinity in the southern parts carries the influence of Atlantic Water inflow with a salinity around 35.1. The mean salinity of the Atlantic inflow is discussed in Sect. 2.3. Surface salinities generally decrease towards the southeastern coast and the surrounding islands, reflecting freshwater input from land (Sect. 2.3), and towards the northern parts due to ice melting.

2.1 Barents Sea volume budget

Inflow of Atlantic Water in the BSO has been well measured since 1997 (Ingvaldsen et al., 2004; Skagseth et al., 2008) and is higher during winter related to the stronger

winds. New data included here compliments the 1997–2001 series up to 2007, and a yearly mean cycle based on 10 years shows a January maximum of 2.8 Sv, falling to an April minimum of 1.1 Sv. The rest of the year it is close to the mean of 1.9 Sv (Table 1). Including the additional Norwegian Coastal Current (NCC) inflow of ∼1.0 Sv (Blindheim, 1989; Ingvaldsen et al., 2004), and 0.3 Sv entering between Svalbard and Franz Josef Land (Maslowski et al., 2004), the inflow to the Barents Sea is roughly 3.2 Sv (Fig. 1). This sets a flushing time for the Barents Sea of 2.5 years, using a mean depth of 230 m and an area of 1.1×10^6 km^2.

The main outflow of ∼2.0 Sv from the Barents Sea takes place between Novaya Zemlya and Franz Josef Land (Gammelsrød et al., 2008), termed the Barents Sea exit (BSX, Fig. 1). Additionally 0.9 Sv leaves in the Bear Island Trench (Skagseth, 2008), and 0.3 Sv leaves through the Kara Gate between Novaya Zemlya and the Siberian coast (Karcher et al., 2003; Maslowski et al., 2004). This is a simplified, but closed, volume flux budget, that will serve as a basis for the ocean transport of heat and salt discussed below. We note that the well measured Atlantic inflow contributes with 2/3, and is thus dominating, but the remaining 1/3 cannot be ignored.

A few more contributions have been estimated, but values are small enough to ignore them in the overall volume budget. This includes input from rivers, rain and sea ice advection amounting to ∼0.04 Sv. These contributions are significant in the Freshwater budget and are discussed in Sect. 2.3. This freshwater input is similar in magnitude to the outflow of dense water produced in the largest fjord around Svalbard (Storfjorden). Inflow of Atlantic Water also occur here, but this water re-circulate south of Svalbard (O'Dwyer et al., 2001). Due to a shallow bank (<100 m depth) with steep topography between Svalbard and Bear Island, this part of the Barents Sea has limited exchange of water with the rest of the sea. This area is therefore also excluded in the "North" area in Fig. 2.

2.2 Heat transport

It was early recognized that the Barents Sea climate is largely controlled by ocean heat transport (Mosby, 1962). Strong correlations between inflow and temperature and the large-scale atmospheric pattern upstream in the Norwegian Sea (the North Atlantic Oscillation) has also been well documented (Loeng et al., 1997; Dickson et al., 2000; Furevik, 2001). Low temperature anomalies in the BSO during the 1980's are also paralleled by low salinity anomalies (Blindheim, 1989; Dickson et al., 2007).

The 1998–2007 mean incoming heat with the Atlantic Water in the Barents Sea Opening is 49.7 TW (Skagseth et al., 2008). Distributed evenly in the entire Barents Sea the inflowing 50 TW would require a net surface heat loss of 38 W/m^2. The heat flux compares to cooling the inflowing 1.9 Sv from 6.4 to 0°C. The mean inflow temperature span the range −4.3–−6.4°C increasing from −5 to −6°C during 1965–2005. Advection of heat has been high in recent years, since 2002 all years have been above 50 TW except 2004 (Skagseth et al., 2008). During the 10 last years variation in ocean volume flux is the main driver of variation in ocean heat transport (Skagseth et al., 2008). The lowest heat flux was measured in 2001 at 30 TW, and corresponded to a relatively low annual mean inflow close to 1.0 Sv (not shown). Figure 3 demonstrates this dependency on a monthly time scale using the constant cooling of 6.4°C. Compared to the calculated heat flux using the individual temperature measurements on each current meter, deviations are generally small, but largest in October at 7 TW. Temperature variations decrease the incoming heat slightly in winter and increase heat flux in summer as one might expect.

Of the total 3.2 Sv inflow to the Barents Sea, the 1.9 Sv through the BSO is, as mentioned, by far the dominant input of heat. The northern inflow of 0.3 Sv (between Svalbard and Franz Josef Land) carries less than 1 TW (Maslowski et al., 2004). How much the remaining 1.3 Sv contributes to the heat transport is not entirely clear.

The NCC of 1.0 Sv has a likely significant, but so far not well quantified, contribution. Based on data from a recent one-year full depth current meter profile in the core of the

NCC, combined with repeated hydrographic profiles the heat transport of the NCC is estimated to 34 TW (Skagseth, 2009). This estimate increases the ocean heat transport to the Barents Sea by ∼50%. The coastal current has been included in freshwater budgets for the Barents Sea earlier (Dickson et al., 2007), but the carried heat has so far to a large extent been unknown. Details on the method for estimated NCC volume, heat, and freshwater content will be described elsewhere (Skagseth, 2009).

The BSX observations from 1991–1992 indicate a heat flux from the Arctic Ocean to the Barents Sea of ∼4 TW (Gammelsrød et al., 2008). When comparing this result with model results (7.4 TW out and 5.6 TW in) the conclusion is that a net volume flux here of 2.0±0.6 Sv has a heat flux not significantly different from zero. The main exiting volume of water, ∼2.0 Sv in BSX, thus leaves at a mean temperature very close to 0°C, and there is little exchange of heat with the Arctic Ocean. The 0.9 Sv leaving in the Bear Island Trench (Skagseth, 2008) does, on the contrary, carry about 12 TW of heat. The last 0.3 Sv leaving in the Kara Gate has less than 1.0 TW according to model results (Maslowski et al., 2004).

In light of the above stated uncertainties some other small heat contributions may be ignored. There is, for example, a contribution from sea ice import from the Arctic estimated to 477 km^2/day (Pavlov et al., 2004), contributing with a heat loss around 1.3 TW, assuming a mean ice thickness of 1 m. In total, the Barents Sea receives 86 TW from the Atlantic inflow and the Norwegian Coastal Current, and looses about 12 TW in the Bear Island Trench, resulting in a net inflow of 73 TW of heat.

2.3 Freshwater budget

In contrast to the heat budget were the inflow is the major contributor, the freshwater budget is more complicated. The Barents Sea lies between the Nordic Seas and the Arctic Ocean, making the Barents Sea freshwater fluxes relevant for both (Serreze et al., 2006; Dickson et al., 2007). The Barents Sea receives significant freshwater input from precipitation and rivers. The net Precipitation-Evaporation balance is roughly ∼0.9 mm/day (Walsh et al., 1998), making the freshwater flux F_{p-e}=13 mSv,

using a Barents Sea area of $1.3\times10^{12}\,m^2$. River inflow is larger, and estimated to $632\,km^3$/year (Dankers and Middelkoop, 2008), equivalent to $F_{river}\sim20$ mSv. These two major contributions are pure freshwater ($S=0$), and thus independent of any choice of reference salinity.

The major balance of the freshwater budget is between the incoming freshwater at the surface, and the removal of freshwater by advection. Following Aagaard and Carmack (1989) and Serreze et al. (2006) a freshwater flux F is based on a volume flux of water V with a salinity S:

$$F = \frac{S_{ref} - S}{S_{ref}} V \,, \tag{1}$$

where we use $S_{ref}=35.0$ as stated in the introduction. The NCC has a mean salinity $S\sim34.4$ and $V=1.0$ Sv (Blindheim, 1989), giving a freshwater flux of $F_{NCC}=17.1$ mSv. Skagseth (2009) estimated the freshwater flux of the NCC to 22.7 mSv by combining current meter and hydrographic data.

The last freshwater source is sea ice import from the Kara Sea and the Arctic Ocean of $477\,km^2$/day (Pavlov et al., 2004) converting to $V=5.5$ mSv. This is a fairly small contribution, assuming 1 m thick ice and a sea ice salinity of $S=5$, we get $F_{seaice}=4.6$ mSv. Zhang and Zhang (2001) model results indicate a larger sea ice volume flux ($339\,km^3$/year) translating into ~10 mSv of freshwater. They also include a significant loss (about 30%) south of Svalbard to the Fram Strait. Zhang and Zhang (2001) found a net precipitation and river runoff much smaller than we have found above, so their net surface freshening is smaller despite the large sea ice contribution.

The total freshwater flux to the Barents Sea is thus of the order 50–60 mSv but how is this freshwater removed? It seems a bit puzzling, but some of it is compensated by the Atlantic inflow. The Atlantic inflow of 1.9 Sv and the higher than mean salinity $S\sim=35.1$ (Skagseth, 2008) is counter-acting the freshwater input with $F_{Atlantic}=-5.4$ mSv. But this is only ~10% of what is needed to balance the input.

The outflow contribution in the BSX is larger with $F_{BSX}=-14.3$ mSv based on 2.0 Sv

and S=34.75 water (Gammelsrød et al., 2008). The return flow in the Bear Island Trench does not contribute when using S_{ref}=35.0 as it has exactly this salinity (Skagseth, 2008). Although the fresh Arctic Water flowing westwards close to Bear Island (the Bear Island Current) is only partly included in this estimate, the current is shallow and its contribution likely small. In any case, the freshwater input is large compared to the removal of freshwater driven by the through-flow. The relative contributions of these sources and sinks would change if we used a different S_{ref}, but we would still need about 35 mSv of freshwater to be removed from the Barents Sea.

The excess 35 mSv of freshwater probably leaves with the 0.3 Sv exiting through the Kara Gate. A balance may be reached by assuming a mean salinity there of S=30.9. The exchange between Svalbard and Franz Josef Land is then assumed to be balanced in freshwater transport. This implies that the 0.3 Sv entering between Svalbard and Franz Josef Land has a salinity close to 35.0 as well.

A rough balance can be achieved between the freshwater associated with through-flow of Atlantic Water ($F_{Atlantic}$+F_{BSX}=19.7 mSv), the freshwater from precipitation-evaporation, the sea ice, and ∼12% of the NCC. The residual freshwater from the NCC, and all the river water remain along the coast, and exit through the Kara Gate.

3 Barents Sea column modelling

The 1DICE column model is forced by monthly mean observations and calculates the horizontally averaged ice thickness and the ocean column below. 1DICE was developed and described in Björk (1989, 1997). A version of 1DICE with an active atmosphere, fluxes from rivers and the Bering Strait, as well as ice export, was applied in Björk and Söderkvist (2002). A simpler setup of 1DICE is used here; a 1 m vertical resolution is used down to a representative Barents Sea depth, the atmosphere is plain forcing. The mean depth of the southern Barents Sea is 253 m, the northern column is 210 m deep. A stable yearly cycle is usually established within 3 years, and model runs were therefore performed over 10 years with a daily time step.

The model mixed layer has instant mixing, and the diffusion below the mixed layer is constant, normally set to K_z=5.0×10^{-6}. As the Barents Sea in most model runs enters a state of convection to the ocean floor during winter, the diffusion plays a role during summer mostly, mixing the warmer mixed layer downwards.

Radiative fluxes are a key controlling factor all over the Arctic. As argued by Eisenman et al. (2007) do many models use the albedo as a "tuning parameter" to correctly model the ice cover. 1DICE is, like any ice-ocean model, sensitive to changes in albedo. A simple thickness dependant bare ice albedo increasing from 0.2 to 0.6 at 2.0 m thickness (Björk and Söderkvist, 2002) is used. For snow a fixed monthly varying albedo is used (Table 1).

1DICE calculates surface heat fluxes; long wave outgoing radiation, latent heat of evaporation, and sensible heat flux, the model grows ice, and mixes heat and salt/freshwater downwards.

3.1 Model forcing

In addition to the forcing from the ocean transport, 1DICE needs atmospheric forcing. This is incoming radiation (shortwave and long wave), air temperature and humidity, mean winds, and snowfall. The monthly mean forcing used is given in Table 1, but is shortly discussed below. The forcing used are horizontally averaged values from the area 12–55° E and 70–80° N, covering the entire Barents Sea. The averaging masks significant gradients in the horizontal forcing fields, but the sensitivity towards this forcing is addressed separately at the end. Data from the ECMWF (ERA 40) and NCAR-NCEP reanalyses have been compared to data from the International Satellite Cloud Climatology Project (version 1, the polar ISCCP, and version 2 the Surface Radiation Budget, SRB).

Solar radiation peaks at 227 W/m^2 in June for the Satellite derived data and ERA 40, whereas NCEP has an additional 100 W/m^2. We have chosen to use the mean of the SRB and Polar ISCCP data. The ERA 40 is almost identical to the Satellite data, but April-May solar radiation is ~10 W/m^2 higher, while July-August is ~20 W/m^2 lower.

November through February is identical for the different sources.

Long wave incoming radiation is high all year, but also peaks in summer. We use the SRB fluxes as they are close to the mean. NCEP is ~20 W/m^2 lower all year, while ERA 40 is ~20 W/m^2 higher in summer, and ISCCP is ~20 W/m^2 higher in winter.

The satellite sources do not give air temperatures, so the values in Table 1 are the means based on ERA 40 and NCEP. They indicate that the southern Barents Sea surface air temperatures gets as cold as −12.2°C in February, and as warm as 3.9°C in August. The means used are close to the mean air temperature from the meteorological stations in the southern Barents Sea; at Bear Island, Hopen Island, Murmansk and southern Novaya Zemlya during winter (1961–1990 normals, http://eklima.met.no and http://www.ncep.noaa.gov). During summer (June–August), the meteorological stations have 2–3°C higher air temperatures. Thus, the reanalysis fields give reasonable estimates, at least in the southern Barents Sea.

The air temperature decrease strongly northwards in the Barents Sea. Two meteorological stations in the northern parts (Victoria Island and Franz Josef Land), are in general 10–12°C colder than the mean based on ERA40 and NCEP during winter, and 3–4°C colder during summer (1961–1990 normals, http://eklima.met.no). The effect of changes in air temperature are examined in sensitivity runs, using both a warmer and colder atmosphere.

Relative humidity of the atmospheric boundary layer is high throughout the year, as one would expect over an ocean. Values increase during summer both for NCEP and ERA 40 from a constant level in winter close to 80%. We use the mean of the two reanalyses, producing the yearly mean of 84%.

Snow fall is applied as direct forcing, but rain is accounted for through the freshwater budget discussed earlier (Sect. 2.3). The ERA 40 data used here indicates ~10 mm/month during winter. Total precipitation from the two meteorological stations indicate a larger precipitation of 31 mm/month for Bear Island and 40 mm/month for Hopen Island (1961–1990 normals, http://eklima.met.no). Snow primarily alters the surface albedo in ice covered situations, where snow albedo decrease from a winter

value of 0.85 to a minimum of 0.64 in July. Values used are identical with those used in Björk and Söderkvist (2002) based on Maykut (1982). Snow albedo is thus always higher than the thickness dependant bare ice albedo in the range 0.2–0.6 (Björk and Söderkvist, 2002).

Both the mean wind and the standard deviation are higher during winter. The values used are based on Børresen (1987). Values are 1955–1981 monthly means from Hind-cast model runs incorporating local met stations. Stronger wind forcing increases vertical heat fluxes and increases turbulent entrainment into the mixed layer, but is not driving the ocean transport.

The yearly mean volume transport used as forcing is 3.2 Sv. Assuming that inflowing water is cooled to 0.0°C, the inflow at 5.6°C carries 73 TW of heat. The major part of this transport is the well sampled Atlantic Water (~2.0 Sv and ~50 TW), as noted above (Table 1 and Fig. 3). The total ocean volume transport used each month as forcing in Table 1 is therefore the sampled Atlantic inflow +1.3 Sv. The individual scatter for each month is large compared to the error using the constant cooling (Fig. 3). Model runs therefore assume the monthly varying volume transport (Table 1) and a constant inflow and outflow temperature.

Sensitivity runs varying the ocean heat transport between 50 TW and 96 TW are included in Sect. 4.1. This variation in ocean heat transport is produced by changing the inflow temperature by ±1°C and the volume transport by ±1 Sv. This sensitivity study thus covers the relatively large uncertainties in the real inflow of heat, including those connected to the Norwegian Coastal Current.

The freshwater forcing used is based on the large scale freshwater budget discussed in Sect. 2.3, and is mimicking the effect of advection on the vertical salinity distribution. The freshwater forcing adds freshwater in the surface layer above 60 m depth. In the deeper layers below 60 m, freshwater is removed (salt is added). This reflects both inflow of (Atlantic) water saltier than the mean, as well as outflow of water fresher than the mean. These two parts balance so that a stable model mean state, without drift in salinity, may be found. The salt budget is closed, so the mean salinity remains

constant. The magnitude of the salt redistribution is scaled by the volume transport and the estimated difference between the inflowing Atlantic Water with salinity close to 35.1 (Skagseth, 2008) and that of the exiting water with salinity of 34.7 (Gammelsrød et al., 2008). Applying only this advection based increase in salinity, without the surface layer freshening, the mean salinity of the Barents Sea increased by 0.63 in 10 years. Freshwater entering and leaving the Barents Sea at the same depth, i.e. freshwater entering with the NCC and exiting in the Kara Gate does not contribute to the salt forcing.

The use of a constant atmospheric forcing in this setup means that no feed-backs involving the atmosphere will be discussed. This relieves us from uncertainties involving cloud cover and corresponding changes in long wave radiation, and allow us to test sensitivity in a straight forward manner.

3.2 Initialisation

Model runs were initiated in August using horizontally averaged profiles of temperature and salinity taken during summer. The averaged profiles are shown in Fig. 4, and are based on available stations in Nilsen et al. (2008) grouped into the "south box" and a "north box" indicated in Fig. 2. We will use the term "box" here, but the vertical dimension is sometimes maintained, so the term "column" could also have been used.

In the south box, data coverage is quite good, with all together 40 000 stations during both winter and summer. In the north box there is 15 000 stations during summer, and 1700 stations during winter. The north box is best covered in its southern parts, particularly during winter. Possible spatial bias has been avoided by subdividing the region into smaller boxes and calculating individual mean profiles therefrom. The overall mean profiles were then based on the small box values. The south box receives all of the ocean heat transport, and looses much of it to the atmosphere. The area over which this heat loss takes place is one of the key parameters of this model approach.

3.3 Southern Barents Sea results – south box

Summer temperature observations (Fig. 4) show a warm surface layer. Surface temperatures may reach 5–8°C, and there are no other temperature maxima below the surface. Downwards there is a gradual decrease to a thick homogeneous lower layer at 2–3°C. Figure 5 shows that the 1DICE model is able to reproduce the main features of a yearly cycle. The surface summer warming is close to observations, and a colder homogeneous water column is established in winter. The model winter mean temperature is 2.83°C, a little warmer than the mean from the observations of 2.03°C.

In summer the warm surface layer is also fresh, and salinities are usually around 34.5. The surface freshening is difficult to reproduce in the same way as the surface summer warming. This reflects uncertainties in surface freshwater balance (rain and advected freshwater in the surface layer). As discussed in Sect. 2.3. The applied salt redistribution works, but only in an approximate way. The freshwater balance is actually quite delicate. The model salinity also becomes homogeneous in winter, whereas the observations from "south box" indicate that it remains slightly stratified in salt.

The area used for the southern box is $(900 \times 400)\,\mathrm{km}^2$, this is ~33% of the Barents Sea area. A perfect fit to any winter temperature may be achieved "tuning" the south box area, and sensitivity towards increasing the "south box" area are included in Sect. 4.2. The observed "south box" winter mean temperature, both horizontally and vertically averaged, is 2.03°C. The similar model mean temperature decreases from 3.22°C in December to 1.7°C in April. The yearly cycle in temperature is thus in good agreement with observations, given the significant temporal and spatial variability of the observations, and the forcing.

The area with higher mean winter surface temperatures than 0°C in Fig. 2 is close to 50% of the Barents Sea, and the difference is thus significant. The area warmer than 0°C has changed over the last decades, and the sensitivity to changes in area of the south box, from the 1970's until today, is included in Sect. 4.4.

The temperature profiles used as validation (Fig. 4) are summer averages from 1

June to 30 September. The model profiles evolves, of course, throughout this period, and it is clear that observations are not evenly distributed in time. For instance, many of the observations are taken in August. Likewise for the winter period 1 December to 30 April, where many of the cruises are conducted in March and April. A perfect match between the average observed profiles and the model profiles is therefore not expected. The maximum observed monthly summer mixed layer temperature of 6.35°C is a good illustration, the model value is a little colder, 5.7°C (Fig. 5). However, in general the 1DICE model is capable of reproducing the major features of the observed annual hydrographic changes in the southern box.

3.4 Northern Barents Sea results – north box

The remaining northern part is the largest area, ~66% of the Barents Sea ($810 \times 900\,km^2$). 1DICE is set up using exactly the same forcing and initialisation as in the south, with one exception, is the ocean heat transport, which is now set close to zero. A value of 2.0 TW is used, comparable to the 3.2 Sv entering at 0.15°C, and exiting at 0.0°C. Results are not sensitive to a small increase of this heat, as long as it is below ~5 TW. Results do not depend on initialisation and a stable yearly cycle is usually entered after three model years.

Figure 5 shows that a very different water column develops in the north, compared to the one in the southern Barents Sea. The yearly cycle is confined to the mixed layer, and shows a shallow heated mixed layer in summer. Summer salinity of this mixed layer is as low as 32.5, caused by significant sea ice melt. From 50 to 100 m the column is at the freezing point, with an increasing salinity. This is similar to the cold halocline found over large areas of the Arctic Ocean. In the lower 100 m temperatures are as warm as 0°C, similar to the Atlantic layer residing below the cold upper layer in the Eurasian basin. At the bottom salinity ends up at 35.2, and the column is so stable that there is no deep convection during winter.

As the upper layer temperature stabilize below 0.0°C, the northern box is "short of" heat referenced to this temperature. This means that the surface fluxes of this

area drives the ocean column towards a state that will be a heat sink using 0.0°C as a reference temperature.

Model salinity decreases more than suggested by observations (Fig. 4) in the upper part of the column. Salinities also increase more in the deeper layers (Fig. 5). This increase is caused by the salt redistribution resembling the advective contribution alone, and is not caused by salt rejected by ice growth. Winter sea ice growth is close to 1 m, but this ice melts again each summer due to the surface fluxes. The salt released during ice growth is counter-acting the other freshwater sources in the top layer, and helps to homogenize the top 60 m during winter.

The model deep salinity continues to increase after 5 years. At 10 years the deep layer ends up at 35.4, but the surface values stabilize. The gradual deep increase is not realistic and points to significant salt fluxes along the northern Barents Sea boundary. The salt redistribution applied here assumes a salinity of 34.75 for the 2.0 Sv exiting in BSX. There are probably additional salt fluxes connected to salt release from ice growth on shallow depth, producing high salinity shelf water S_w>34.8 escaping close to bottom.

3.5 Barents Sea surface heat loss

The Barents Sea has now been divided in two boxes. The south box gets all the ocean heat, the northern box only receives significant heat at the surface. The two averaged water columns are largely in line with the observed mean profiles from the boxes, confirming that this simple division is meaningful.

The transported 73 TW of ocean heat arriving in the BSO is lost to the atmosphere. But there is also additional heat arriving as short wave radiation during summer, the yearly mean model solar heating is 26 TW for the southern box, and 33 TW for the northern box. The two boxes receives the same solar radiation per m^2 (Table 1), but the northern box is 66% of the area, the southern only 33%. The difference in area is compensated by difference in sea ice cover, creating a solar input to the boxes of similar magnitude.

For the northern box the sensible heat flux is also positive during summer, caused by air temperatures of 2–3°C above the colder surface water. As mention earlier the meteorological stations from the northern Barents Sea revealed air temperatures 2–3°C lower than the forcing applied here during summer, indicating that the sensible heat flux might be close to zero. Net long wave and latent heat fluxes are always negative both in the north and south. In the north the surface fluxes are close to being in balance, so the mean total heat flux is −5 TW. Given that the yearly cycle varies between a loss of 80 TW and a gain of 120 TW (not shown), −5 TW is effectively zero. This means that nearly all of the ocean heat transport must be given up to the atmosphere over the southern 33% of the Barents Sea area.

The model average heat loss from the southern Barents Sea is 67 TW as shown in Fig. 6. This is 6 TW less than the ocean heat transport, and indicates a slow warming. This is confirmed in model profiles, where the mean temperature increases from 3.36°C at initialisation, to 3.51°C in year 6, but the difference is too small to be visible in Fig. 7. As noted in Sect. 2.2 are there substantial year to year fluctuations in the Atlantic inflow, ranging from 30 to 60 TW.

The net heat loss is partitioned into long wave, sensible, and latent heat fluxes (Fig. 6). Long wave radiation has a mean loss of 23 TW. There is 32 TW of latent heat loss, and 39 TW of sensible heat loss (Table 2). The yearly cycle is smaller in the south, caused by the smaller area, and the maximum net heat gain is 26 TW during summer. All three heat loss contributions peak during winter when there is no solar heating, causing the maximum heat loss of 150 TW. There are some days with a very thin ice cover during the winter. This ice quickly melts again as the oceanic heat is mixed upwards. The small portions of sea ice created by 1DICE lowers the heat fluxes during late winter, causing the reduced loss from ∼150 TW to ∼100 TW between 4.4 and 4.6 years in Fig. 6.

The different heat fluxes are summarized in Table 2. The total heat loss from the 2 Barents boxes used in the 1-D model add up to 70.2 TW, close to the transported 73 TW of heat by the ocean. The agreement is superficial in the way that the 73 TW

was added to the southern box, but the northern box is demanding ~3 TW totally on its own. The southern box reaches a close to stable state with the heat loss of 67.2 TW.

4 Discussion

The transported ocean heat to the Barents Sea is lost as long wave radiation, as well as latent and sensible heat fluxes. The simplified picture of the Barents Sea as two boxes is largely consistent with the earlier estimates of Simonsen and Haugan (1996) and Zhang and Zhang (2001). For all components in Table 2 the 1-D results presented here are found between the two earlier estimates.

In 1DICE the two largest contributions to the heat flux, the incoming short wave and the outgoing long wave, nearly cancel in the annual mean (Table 2). Such a balance is not found by Simonsen and Haugan (1996) and Zhang and Zhang (2001). Sensible and latent heat losses are significantly smaller than Simonsen and Haugan (1996), but larger than Zhang and Zhang (2001). In the northern box sensible heat fluxes do not contribute to the ocean heat loss. Our results show infact a small warming of the ocean, caused by the surface waters being close to freezing much of the year. The observed air temperature from the northern Barents Sea is of course colder than the mean air temperature for the whole sea, so this ocean warming may be an artifact of the 1-D approach.

The 1DICE model is a good tool to study sensitivity because it is computationally cheap and quick. The monthly mean forcing is applied repeatedly for all years, and usually a stable situation is established during 3 years, as illustrated in Fig. 7.

4.1 Ocean heat transport variability

The ocean heat transport to the Barents Sea has varied during the last 10 years (Skagseth et al., 2008). In order to explore this dependence further the transport was varied from the mean state of 3.2 Sv and 5.6°C used in the "south box" run. Fig-

ure 7 shows how the depth-averaged temperature varies through the 6 first years in the "south box" run described in Sect. 3.3. Note that the same initial ocean column will be used for all sensitivity runs. Usually 1DICE also settles into a new stable yearly cycle after about 3 years, comparable to the Barents Sea flushing time of 2.5 years. The observed winter mean value of 2.03°C is found in the middle of the model results through the winter. The winter temperature is quite homogeneous, and is therefore a good indicator of available heat (Fig. 4).

Four runs are presented in Table 2 varying the ocean heat transport; "Morewater", "Lesswater", "Warmwater", and "Coldwater". As mentioned in Sect. 2.2 has fluctuation in volume flux governed ocean heat transport variability the last 10 years. In "Morewater" the monthly mean ocean volume transport (Table 1) has been increased with 1 Sv for all months through the year, giving a yearly mean of 4.2 Sv. This creates an ocean heat transport of 96 TW. In the same manner "Lesswater" has a yearly mean ocean transport of 2.2 Sv, and a heat transport of 50 TW.

In the "Morewater" run the 1 Sv increased ocean heat transport (96 TW) produces a warmer winter column as expected. Figure 7 shows that the summer maximum mean temperature reaches above 5°C the second model summer. After model year 2 a new stable yearly cycle is established, and mean surface fluxes are given in Table 2. The change is significant but moderate, and the warming during summer is larger than during winter. The yearly cycle is increased in magnitude with 0.75°C as shown in Fig. 7.

With an ocean heat transport lowered by 1 Sv (to 50 TW) in the "Lesswater" run, the Barents Sea water column cools by ~2°C (Fig. 7). The response is more continuous than for the "Morewater" run, and a gradual cooling appears throughout the 10 model years. After 6 years the winter mean temperature reaches 0°C in winter. The accompanying heat fluxes are included in Table 2. Summer temperatures also cool down in the deep, but the solar radiation still warm up the surface layer to around 4°C (not shown).

The effect of removing 1 Sv in the "Lesswater" run is thus larger than adding 1 Sv in the "Morewater" run. This probably reflects both the importance of the ocean heat

transport to the Barents Sea and that the atmospheric heat loss has a damping effect on fluctuations in the transported heat. If the heat transport decrease, the model immediately starts to cool down. The real ocean would probably respond in this way too, but in addition change the area of the box. On the other hand, when the heat transport increase, the heat loss during winter will also increase. Figure 7 shows that yearly temperature cycle increases with increasing ocean transport, and that the summer temperatures changes the most. The heat transport driven changes are thus dampened more during the cold season than during the warm season.

In "Warmwater" the inflow temperature has been increased by 1°C, this increases the ocean heat transport from 73 TW to 86 TW. This heat transport is mid way between the "south box" and "Morewater" runs, and the total model heat loss becomes 82.5 TW. The other surface fluxes are included in Table 2.

The effect on mean winter and summer temperatures is plotted in Fig. 8, together with the other sensitivity runs. The variation in temperature are clearly damped in the Barents Sea. The increase of 1°C at the boundary results in an increase of ~0.75°C in the mean. Such a damping of the oceanic signals in the Barents Sea has earlier been observed by Schauer et al. (2002) and Ingvaldsen and Gjøsæter (2009). Although the effect of increasing the temperature with 1°C is smaller than the effect of increasing the volume flux by 1 Sv, it gives a highly significant contribution (Fig. 8). While the volume flux has a strong variation on inter-annual time scales (Ingvaldsen et al., 2004), the inflowing temperature shows long-term trends and has increased by more than a degree since the late 1970s (Skagseth et al., 2008). Thus variability in the inflow temperature is likely to be highly important on longer time scales.

The effect of decreasing inflow temperature by 1°C is shown in the "Coldwater" run, lowering the ocean heat transport to 60 TW (Fig. 8). Again we find a damping in the Barents Sea, the mean winter and summer temperatures are lowered by less than the 1°C decrease of the inflow. As in the "Lesswater" run the damping is stronger during winter, than during summer. The mean surface fluxes are tabulated in Table 2.

Using a smaller transport than 50 TW of heat creates some unexpected results.

40 TW of ocean heat produces a surface heat loss around 12.5 TW, much smaller than the added heat. This means that the Barents Sea water column heats up with about 27 TW, producing a mean temperature around 5°C in 4 years. In this situation the cooling during winter is not strong enough to erode the fresher surface mixed layer established during summer. Consequently, there is no homogeneously mixed water column during winter, and the warm water remains isolated from the cold atmosphere. The winter convection and cooling reach about 50 m depth, so temperature remains around 0°C in the top 50 m. After four model years results become unrealistic and points to the limitation of the 1-D model and the added salt redistribution.

Despite the limitations of the 1-D approach, the results indicate a lower limit on heat transport to the Barents Sea that would start a transition into a new steady state. This new steady state has the same qualitative properties as the Arctic, with a warmer Atlantic layer below a colder, and stable, upper layer.

4.2 Changes in cooling area

The main balance in the 1DICE model is between the ocean heat transport and the area available for cooling this water. Increasing the size of the area in "box south" leads to a larger heat loss.

The northern and southern box is driven by exactly the same monthly mean forcing, and the model runs therefore support a few new balances within the Barents Sea. The northern part gets little ocean heat transport and naturally enters a state that produce sea ice every winter, has an upper water column at the freezing point, and a small ocean to air heat loss of ~3 TW. Such an ocean column covers a relatively large part of the Barents Sea, in our model it is about 66% of the area.

The southern box, driven by exactly the same surface forcing, enters a totally different regime because of the transported ocean heat. The area used in this model, 33% of the Barents Sea, produces a fairly good agreement with the observed mean temperatures. The long-term mean area warmer than 0°C during winter (Fig. 2) is however close to 50% of the Barents Sea. If a larger area is used for the southern box keep-

ing the transported ocean heat at 73 TW, the temperatures in the box decrease. Two runs using an increased "box south" area to 40% and 50% of the Barents Sea, give decreased mean temperature of 1–2.5°C (Fig. 8).

The reduced temperature could indicate, for example, uncertainties of the extracted monthly forcing. They could also indicate limitations of the simple column model approach, or that the main heat loss actually takes place over an area significantly smaller than the 50%. The cooling area could be defined in many ways; water warmer than some limitation, the position of Polar Front, or the ice free area. Regardless of the definition large changes in the cooling area occur regularly in the Barents Sea (e.g. Loeng, 1991; Vinje, 2001; Sorteberg and Kvingedal, 2006; Ådlandsvik, 2009). More important than finding the exact area corresponding to the mean situation, is finding how changes in the cooling area relates to changes in the ocean heat transport and how this affects the balance in the region.

Over the period 1997–2006 the volume flux in the BSO increased by 1 Sv and the inflow temperature increased by 1°C (Skagseth et al., 2008). According to Fig. 8 this should cause the winter and summer mean temperature of the southern Barents Sea to increase significantly. The response for mean temperature towards variation in ocean heat transport is close to linear, and observations suggest adding the "Morewater" and "Warmwater" runs, i.e. a warming of around 2°C. Such a large general warming has not been observed. However, a simultaneous increase in cooling area of 10–20% would reduce the temperature increase to 0.5–1°C which is more in line with the observations.

4.3 Atmospheric warming and cooling

In the 2000's the Barents Sea region atmosphere has experienced a significant atmospheric warming (Zhang et al., 2008). Winter observations from Bjørnøya (not shown) has increased from around −8°C for the 1960–1990 period to around −2°C for the 2005–2008 period. How much is this warming affecting the Barents Sea? To investigate this the mid winter air temperature was increased from −12°C to −8°C. For the other months the air temperature was increased by 1°C (see Air temperature in Ta-

ble 1).

For Barents Sea temperatures, the effects are small as shown in Fig. 8. The winter mean temperature increases with 0.22°C. The warmer air has other significant impacts, on the sea ice thickness in the northern Barents Sea, for example, but we rest that issue here now.

In this study we used mean air temperatures from the ERA 40 and NCEP reanalysis covering the entire Barents Sea. These air temperatures were found to be comparable to means from met stations in the southern Barents Sea. Our 1DICE model nevertheless reproduce a cold northern ocean, with small air-sea sensible and latent heat fluxes. The inter-annual variability in the air temperatures are large, and to evaluate the effect of decreased winter air temperatures, a sensitivity run was performed for the southern box using mean temperatures based on available meteorological stations in the northern Barents Sea. These stations have a mid winter air temperature around −25°C. The effect on the Barents Sea mean temperatures are modest; a cooling of 0.75–1°C is small, considering the extreme cold air (Fig. 8).

The results indicate that air temperatures have a modest effect on the overall heat loss, especially compared to the cooling area.

4.4 Decadal variability

Hydrographic data back to the 1970's was assembled and used to produce the mean hydrographic climatology of the NISE data set (Nilsen et al., 2008). Our aim was originally to also present decadal estimates of the variability in the Barents Sea heat storage. Some sections are available on a regular basis back to 1980, like the one across the BSO (Furevik, 2001). The Russian Kola section is also available back to about 1910, and bear a multi-decadal signal similar to the Atlantic Multidecadal Oscillation (Skagseth et al., 2008). But in general the data available, in addition to these sections, is quite limited. We have therefore found that mean temperatures over decadal time frames have little value, and have questionable representativity.

The minimum yearly mean temperature of the Atlantic layer in the BSO was 4.3°C

in 1978–1979, and the maximum was 6.4°C in 2006 (Skagseth et al., 2008). This range probably carries a general warming trend, and the normal decadal variability in temperature is around ±0.5°C. In line with our findings above the deeper layers in the BSO have the larger variability, and the warming and cooling episodes of the 1980's are generally stronger at 400 m than they are closer to the surface (Furevik, 2001).

Given that decadal values of temperature could be estimated for the southern Barents Sea, our model setup could relate observed changes in mean temperatures to likely ocean heat transport as shown in Fig. 8. An observed change in cooling area could also be compared to the mean temperature, and the related ocean heat transport. For now we just summarise that the observed decadal variability is around ±0.5°C. This is a significantly smaller variability than one could expect based on the observed changes in inflow during the last decade. Figure 8 therefore indicates that the Barents Sea has responded to increasing ocean heat transport by increasing the area where the heat loss takes place.

5 Conclusions

An updated synthesis indicates that the ocean volume transport to the Barents Sea is 3.2 Sv. This flow carries 73 TW of heat, and removes the excess freshwater entering by rain, sea ice, and 1/2 of the Norwegian Coastal Current. The Atlantic Water transports 50 TW of heat in 1.9 Sv of water.

Horizontally averaged profiles of temperature and salinity shows that the Barents Sea may be qualitatively divided into two columns. The northern column is stratified in salinity, and has a surface layer close to the freezing point during winter. The southern column mixes fully during winter and is re-stratified every summer by the solar heating.

A column model is used to reproduce these two regions of the Barents Sea. Yearly mean monthly forcing is applied, and usually a new stable state is established within 3–5 years. The surface summer warming and freshening takes place both in the northern and southern Barents Sea, while the deep convection in winter only appears in the

south. Model results thus reproduce the mean summer and winter profiles of temperature in a good way, but the average salinity profiles are more sensible to the freshwater forcing.

The heat transported to the southern Barents Sea is lost by sensible and latent heat fluxes. In this area short wave and long wave radiation nearly cancel over a year, with a small net ocean warming of 3 TW. A stable yearly cycle in mean temperature from a minimum of 1.8°C in late winter to a maximum of 4.1°C in late summer is established in the south.

The northern Barents Sea receives little ocean heat, and ∼1 m of sea ice grows and melts every year. The yearly mean total heat loss is around 5 TW in the north. The combined solar and long wave radiation has the same small positive contribution as in the south (3 TW), but in the north sensible and latent heat fluxes are also small.

The column model shows a linear relation between ocean heat transport and the mean temperature. For the southern Barents Sea an ocean warming of +1°C, corresponding to an increased heat transport of 13 TW, would result in a ∼0.8°C warming. The mean temperature also depends on the cooling area, and this increased ocean heat transport can be compensated by increasing the cooling area by 10%.

In recent years a northward shift of the Polar Front, a related northward shift of the winter ice edge, and an increased ocean heat transport (Skagseth et al., 2008) has been observed. Our model approach separates the two mechanisms, and indicate that if this expansion in cooling area did not occur, the warming would have been much larger.

The Barents Sea is an effective and robust ocean cooler. The observed variability in volume and inflow temperature is large, but the variability in mean temperature, or stored heat, is low. Our results therefore indicate that the ocean heat transport modulates both the Barents Sea mean temperature, and the area over which cooling occurs. When the heat transport increases, the warm water spreads further into the sea, causing cooling over a larger area. This is consistent with a retreat of the sea ice cover as suggested by Sorteberg and Kvingedal (2006), and a temperature that varies

OSD
6, 1437–1475, 2009

in phase over the southern Barents Sea (Ingvaldsen et al., 2003).

As a result, the water leaving the Barents Sea toward the Arctic Ocean has temperatures close to 0°C. The northern Barents Sea does not contribute significantly to the cooling, but acts as a buffer into were the southern effective cooling area may expand.

Acknowledgements. This work was completed as a part of the Polar Climate and Heat Transport (Pocahontas) project, funded by the Research Council of Norway. This is publication A237 from the Bjerknes Centre for Climate Research. The atmospheric forcing data were provided by A. Sorteberg (Geophysical Institute, University of Bergen), but he was, unfortunately, to busy to join in at the writing stage. Thanks to E. Falck for improving the language. The ocean temperature and salinity data were provided by: The Marine Research Institute, Iceland; Institute of Marine Research, Norway; the Faroese Fisheries Laboratory; the Arctic and Antarctic Research Institute, Russia, and Geophysical Institute, University of Bergen, Norway, through the NISE project.

References

Aagaard, K. and Carmack, E.: The role of sea ice and other fresh water in the Arctic cictulation, J. Geophys. Res., 94, 14485–14489, 1989. 1439, 1444

Ådlandsvik, B.: The Polar Front in the Barents Sea, in preparation., 2009. 1458

Björk, G.: A one-dimensional time-dependant model for the vertical stratification of the upper Arctic Ocean, J. Phys. Oceanogr., 19, 52–67, 1989. 1445

Björk, G.: The relation between ice deformation, oceanic heat flux, and the ice thickness distribution in the Arctic Ocean, J. Geophys. Res., 102, 18 689–18 698, 1997. 1445

Björk, G. and Söderkvist, J.: Dependence of the Arctic Ocean ice thickness distribution on the polward energy flux in the atmosphere, J. Geophys. Res., 107(C10), 3173, doi:10.1029/2000JC000723, 2002. 1445, 1446, 1448

Blindheim, J.: Cascading of Barents Sea bottom water into the Norwegian Sea, Rap. Proces., 226, 49–58, 1989. 1441, 1442, 1444

Børresen, J. A.: Wind atlas for the North Sea and the Norwegian Sea, Tech. Rep., The Norwegian Meteorological Institute, Norwegian University Press, Oslo, ISBN:82-00-35276-5, 1987. 1448

Dankers, R. and Middelkoop, H.: River discharge and freshwater runoff to the Barens Sea under present and future climate conditions, Clim. Change, 87, 131–153, doi:10.1007/s10584-007-9349-x, 2008. 1444

Dickson, R., Osborn, T., Hurrell, J., Meincke, J., Blindheim, J., Ådlandsvik, B., Vinje, T., Alekseev, G., and Maslowski, W.: The Arctic Ocean response to the North Atlantic oscillation, J. Climate, 13, 2671–2696, 2000. 1442

Dickson, R., Rudels, B., Dye, S., Karcher, M., Meincke, J., and Yashayaev, I.: Current estimates of freshwater flux through Arctic and subarctic seas, Prog. Oceanogr., 73, 210–230, 2007. 1439, 1442, 1443

Eisenman, I., Untersteiner, N., and Wettlaufer, J.: On the reliability of simulated Arctic sea ice in global climate models, Geophys. Res. Lett., 34, L10501, doi:10.1029/2007GL029914, 2007. 1446

Furevik, T.: Annual and interannual variability of Atlantic Water temperatures in the Norwegian Seas: 1980–1996, Deep-Sea Res., 48, 383–404, 2001. 1442, 1459, 1460

Gammelsrød, T., Leikvin, Ø., Lien, V., Budgell, W., Loeng, H., and Maslowski, W.: Mass and heat transports in the NE Barents Sea: Observations and models, J. Marine Syst., 7(1–2), doi:10.1016/j..marsys.2008.07.010, 2008. 1441, 1443, 1445, 1449

Ingvaldsen, R. and Gjøsæter, H.: Impact of climate variability, stock size and age composition on the spatial distribution of Barents Sea capelin, ICES J. Mar. Sci., submitted, 2009. 1456

Ingvaldsen, R., Loeng, H., Ottersen, G., and Ådlandsvik, B.: Climate variability in the Barents Sea during the 20th century with focus on the 1990s, 219, pp. 160–168, ICES Marine Science Symposia, 2003. 1462

Ingvaldsen, R., Asplin, L., and Loeng, H.: The seasonal cycle in the Atlantic transport to the Barents Sea during the years 1997–2001, Cont. Shelf Res., 24, 1015–1032, 2004. 1440, 1441, 1456

Karcher, M., Kulakov, M., Pivovarov, S., Schauer, U., Kauker, F., and Schlitzer, R.: Atlantic water flow to the Kara Sea: comparing model results with observations, in: Proceeding in Marine Science, Siberian River Run-off in the Kara Sea: Characterisation, Quantification, Variability and Environmental Significance, edited by: R. Stein, R., Fahl, K., Futterer, D., and Galimov, Elsevier Science B.V., 47–69, 2003. 1441

Loeng, H.: Features of the physical oceanographic conditions of the Barents Sea, Polar Res., 10, 5–18, 1991. 1458

Loeng, H., Ozhigin, V., and Ådlandsvik, B.: Water fluxes through the Barents Sea, ICES J. Mar.

Sci., 54, 310–317, 1997. 1442
Maslowski, W., Marble, D., Walczowski, W., Schauer, U., Clement, J. L., and Semtner, A. J.: On climatological mass, heat, and salt transports through the Barents Sea and Fram Strait from a pan-Arctic ice-ocean model simulation o, J. Geophys. Res., 109, C03032, doi:10.1029/2001JC001039, 2004. 1441, 1442, 1443
Maykut, G.: Large scale heat exchange and ice production in the central Arctic, J. Geophys. Res., 87, 7971–7984, 1982. 1448
Mosby, H.: Water, salt and heat balance of the North Polar Sea and the of the Norwegian Sea, Geofysiske Publikasjoner (Geophysica Norvegica), 24, 289–313, 1962. 1440, 1442
Nilsen, J., Hátún, H., Mork, K., and Valdimarsson, H.: The NISE dataset, Technical Report 08-01, Faroese Fisheries Laboratory, Box 3051, Tórshavn, Faroe Islands, 2008. 1440, 1449, 1459
O'Dwyer, J., Kasajima, Y., and Nøst, O.: North Atlantic water in the Barents Sea opening, 1997 to 1999, Polar Res., 2, 209–216, 2001. 1441
Pavlov, V., Pavlova, O., and Korsnes, R.: Sea ice fluxes and drift trajectories from potential pollution sources, computed with a statistical sea ice model of the Arctic Ocean, J. Marine Syst., 48, 133–157, 2004. 1443, 1444
Schauer, U., Loeng, H., Rudels, B., Ozhigin, V., and Dieck, W.: Atlantic Water flow through the Barents and Kara Seas, Deep-Sea Res. Part I, 49, 2281–2298, 2002. 1439, 1456
Serreze, M., Barrett, A., Slater, A., Woodgate, R. A., Aagaard, K., Lammers, R. B., Steele, M., and Moritz, R.: The large-scale freshwater cycle of the Arctic, J. Geophys. Res., 111, C11010, doi:10.1029/2005JC003424, 2006. 1443, 1444
Serreze, M., Barrett, A., Slater, A., Steele, M., Zhang, J., and Trenberth, K.: The large-scale energy budget of the Arctic, J. Geophys. Res., 112, D11122, doi:10.1029/2006JD008230, 2007. 1438
Simonsen, K. and Haugan, P. M.: Heat budgets for the Arctic Mediterranean and sea surface heat flux parameterizations for the Nordic Seas, J. Geophys. Res., 101, 6553–6576, 1996. 1454
Skagseth, Ø.: Recirculation of Atlantic water in the western Barents Sea, Geophys. Res. Lett., 35, L11606, doi:10.1029/2008GL033785, 2008. 1441, 1443, 1444, 1445, 1449
Skagseth, Ø.: Wind impact on the transports by the Norwegian Coastal Current in the Barents Sea, in preparation, 2009. 1443, 1444
Skagseth, Ø., Furevik, T., Ingvaldsen, R., Loeng, H., Mork, K., Orvik, K., and Ozhigin, V.: Vol-

ume and heat transport to the Arctic Ocean via the Norwegian and Barents Seas, in: Arctic – Subarctic Ocean Fluxes, edited by: Dickson, R., Meincke, J., and Rhines, P., Springer Verlag, Dordrecht, The Netherlands, 45–64, 2008. 1440, 1442, 1454, 1456, 1458, 1459, 1460, 1461

Sorteberg, A. and Kvingedal, B.: Atmospheric Forcing on the Barents Sea Winter Ice Extent, J. Climate, 19, 4772–4784, 2006. 1458, 1461

Vinje, T.: Anomalies and trends of sea-ice extent and atmospheric circulation in the Nordic Seas during the period 1865–1998, J. Climate, 14, 255–267, 2001. 1458

Walsh, J., Kattsov, V., Portis, D., and Meleshko, V.: Arctic precipitation and evaporation: model results and observatinal estimates, J. Climate, 11, 72–87, 1998. 1443

Zhang, X. and Zhang, J.: Heat and freshwater budgets and pathways in the Arctic Mediterranean in a coupled ocean/sea-ice Model, J. Oceanogr., 57, 207–234, 2001. 1444, 1454

Zhang, X., Sorteberg, A., Zhang, J., Gerdes, R., and Comiso, J.: Recent radical shifts of atmospheric circulations and rapid changes in Arctic climate system, Geophys. Res. Lett., 35, L22701m doi:10.1029/2008GL035607, 2008. 1458

Table 1. Monthly mean forcing for the Barents Sea. Values are means over each month and over the Barents Sea area. Atlantic inflow is updated from Ingvaldsen et al. (2004) and Skagseth et al. (2008). The other data included are based on existing estimates cited in the text.

Parameter	Jan	Feb	Mar	Apr	May	Jun	Jul	Aug	Sep	Oct	Nov	Dec	Mean
Solar radiation W m^{-2}	0.0	1.8	33.7	106.2	183.4	227.4	203.3	133.9	55.2	9.4	0.1	0.0	79.5
Long wave in W m^{-2}	224.3	226.9	232.7	239.4	267.4	286.4	299.0	293.5	281.1	258.6	239.0	227.9	256.4
Air temp. °C	−11.6	−12.2	−9.8	−8.6	−2.6	1.6	3.5	3.9	2.5	−2.4	−6.8	−10.0	−4.4
Relative humidity %	80	81	81	80	81	87	91	88	85	80	81	80	84
Snow fall mm/day	11.1	9.9	7.8	6.6	3.9	1.2	0.0	0.0	1.5	7.2	8.7	11.1	5.8
Snow albedo	0.85	0.84	0.83	0.81	0.82	0.78	0.64	0.69	0.84	0.85	0.85	0.85	0.80
Mean wind m/s	9.3	9.2	8.7	7.4	6.1	5.8	5.2	5.7	6.7	7.6	8.6	9.0	7.4
Wind std deviation m/s	4.7	4.7	4.2	3.8	3.4	3.2	2.9	3.2	3.6	4.1	4.3	4.3	3.9
Atlantic volume transport (Sv)	2.75	2.30	2.05	1.12	1.69	1.85	1.64	1.95	1.71	1.71	2.14	1.85	1.90
Ocean volume transport (Sv)	4.05	3.60	3.35	2.42	2.99	3.15	2.94	3.25	3.01	3.01	3.44	3.15	3.20

OSD
6, 1437–1475, 2009

Table 2. Mean yearly surface heat fluxes for the Barents Sea in TW. The 1-D total is our best estimate for the total Barents Sea. The "north box" contribution is quite small, and the major heat loss occurs in the "south box". The eight sensitivity runs are included at the bottom of the table, and are all performed over the "south box" area.

Heat flux	Total	Shortwave	Long wave	Sensible	Latent
Simonsen and Haugan	−135.2	69.9	−54.9	−85.0	−65.2
Zhang and Zhang	−39.3	78.1	−37.2	−17.4	−20.2
1-D total	−70.2	51.1	−45.0	−34.5	−41.8
North box	−3.0	25.1	−22.5	4.4	−10.0
South box (73 TW)	−67.2	26.0	−22.5	−38.9	−31.8
Morewater (+1 Sv, or 96 TW)	−94.6	26.4	−26.0	−53.0	−42.0
Lesswater (−1 Sv, or 50 TW)	−41.3	25.1	−19.0	−25.3	−22.1
Warmwater (+1°C, or 86 TW)	−82.5	26.3	−24.5	−46.8	−37.6
Coldwater (−1°C, or 60 TW)	−51.3	25.6	−20.4	−30.5	−25.9
Warm Air	−73.2	26.3	−25.6	−39.3	−34.7
Cold Air	−63.2	23.7	−11.3	−50.9	−24.7
Larger area (40%)	−51.6	25.5	−20.4	−30.7	−26.0
Largest area (50%)	−38.4	25.0	−18.6	−23.7	−21.1

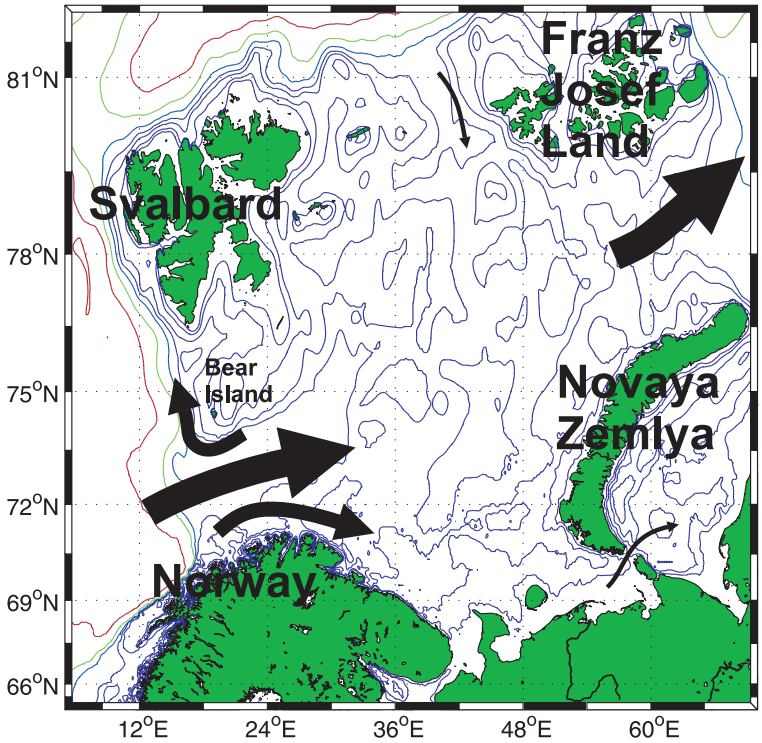

Fig. 1. The Barents Sea and surrounding islands. Mean flow is sketched based on various sources described in the text, and arrows are scaled using 0.1 Sv=1.0 pt. Depth contours are plotted for 50 m, 100 m, 200 m, 300 m, 500 m, 1000 m, and 2000 m.

OSD
6, 1437–1475, 2009

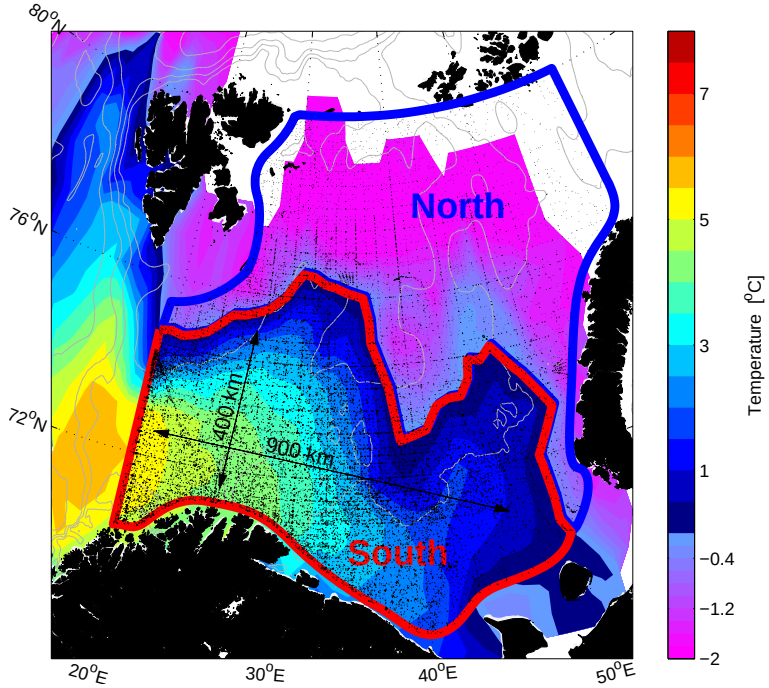

Fig. 2. Mean temperature during winter at 10 m depth (data from Nilsen et al., 2008). Positions of the 55 000 stations used is shown with black dots. The Barents Sea is divided into two boxes; "North" and "South" defined by the mean winter 0°C surface isotherm.

OSD
6, 1437–1475, 2009

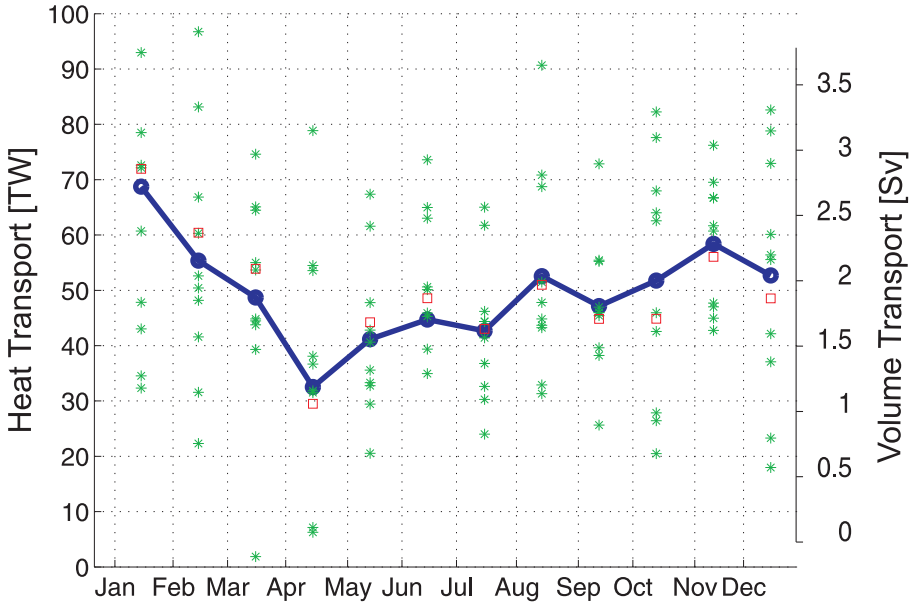

Fig. 3. Atlantic heat transport through the Barents Sea Opening. Blue solid line shows the overall yearly mean cycle of heat transport referenced to 0°C for the 1997–2008 data. Green asterisks show individual monthly heat transport values. The mean Atlantic volume transport (Table 1) is plotted as red squares in relation to the right vertical axis, but also shows the related yearly cycle in heat transport.

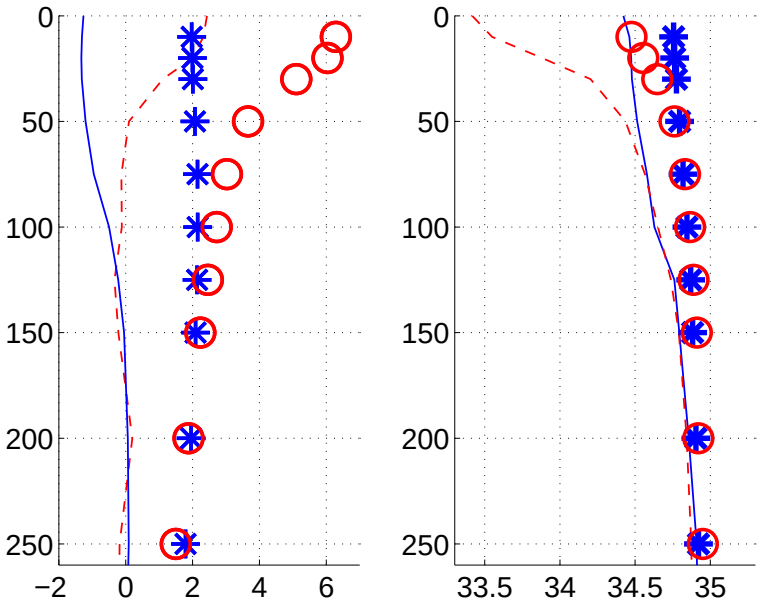

Fig. 4. Mean temperature and salinity in the boxes as obtained from observations. Summer data (June through September) are plotted in red, winter data (December through April) are plotted in blue. Data from "box south" are plotted using circles and asterisks, and for "box north" using solid and dashed lines.

OSD
6, 1437–1475, 2009

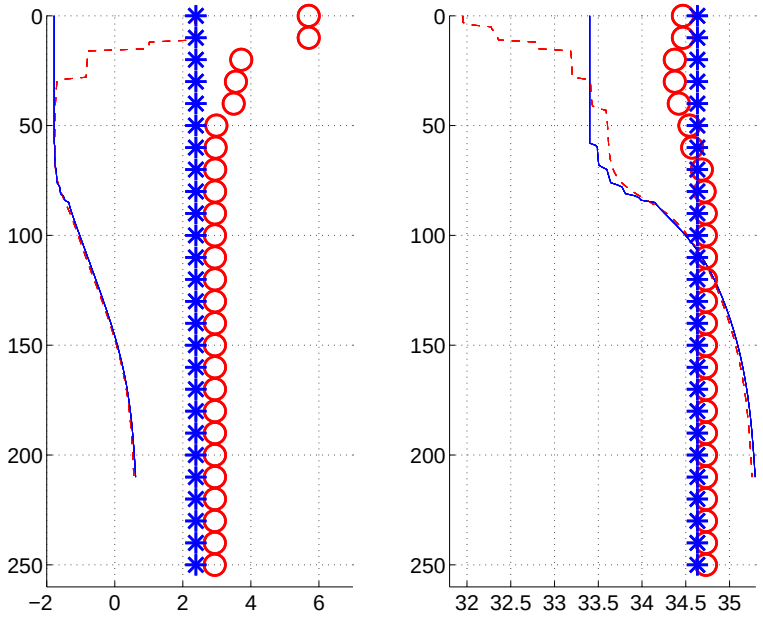

Fig. 5. Profiles of Barents Sea model temperature and salinity. Summer means (June–September) are plotted in red, winter (December–April) in blue. Results for box South are plotted using circles and asterisks, and for box North using solid and dashed lines.

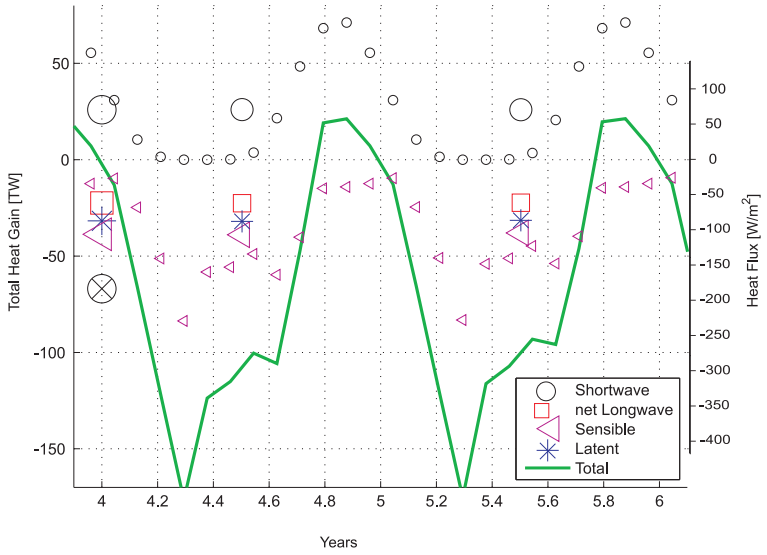

Fig. 6. Model heat gain for the southern Barents Sea. Values are plotted in Terra Watt (1 TW=10^{12} W) for year 4 and 5. The overall total heat gain is −67 TW, indicating a heat loss comparable to the ocean transport (plotted at 4.0 years as ⊗). During summer the total heat gain is positive, peaking at 26 TW. Short wave radiation and sensible heat flux is plotted every month, the other contributions are included as annual means only at year 4.5 and 5.5. Values at year 4.0 (larger symbols) are means over year 2 to year 8. The extra axis to the right is added to aid comparison with other surface flux estimates.

OSD
6, 1437–1475, 2009

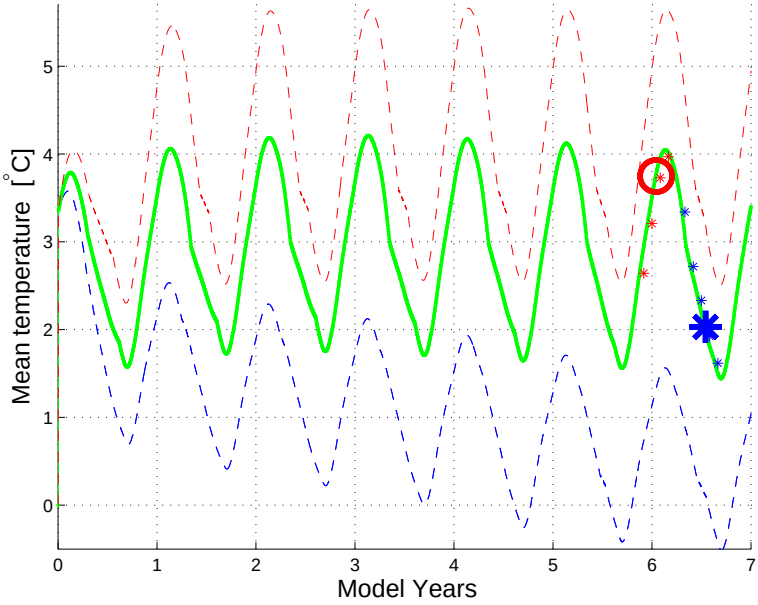

Fig. 7. Depth averaged model temperature of the southern Barents Sea. Results using the deduced mean ocean heat transport of 73 TW are shown by a green solid line. Individual months during year 6 are plotted for summer (June–September) as red asterisks, and winter (December–April) as blue. The observed winter mean (large blue asterisk) and summer mean (large red circle) is also plotted in year 6. Results using a 1 Sv decreased ("Lesswater" run, dashed blue line, 50 TW) and a 1 Sv increased ocean heat transport ("Morewater" run, red dash-dotted line, 96 TW) are also shown.

OSD
6, 1437–1475, 2009

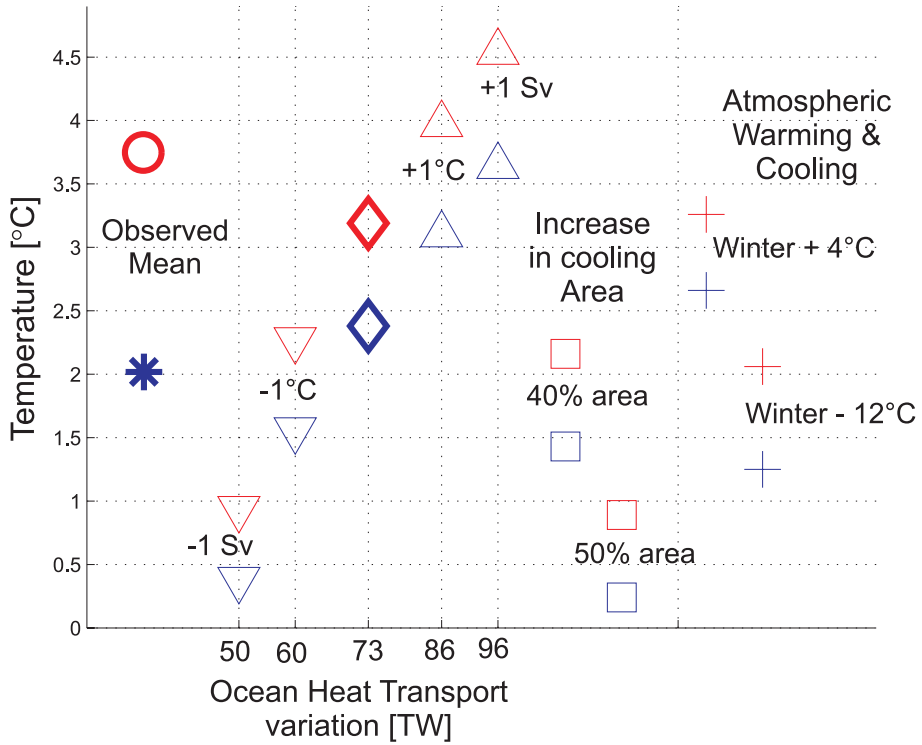

Fig. 8. Sensitivity of the depth averaged model winter and summer temperatures of the southern Barents Sea. Summer values are red, winter values are blue. The different model runs are described in the text, and are the same as those in Table 2. Observationally based values are found to the left (Summer – ∘, Winter – ∗), and the standard run "south box" value are plotted as diamonds.

OSD
6, 1437–1475, 2009